Type of the Paper (Article, Review, Communication, etc.)

Maximum Power Point Tracking for Brushless DC Motor Driven Photovoltaic Pumping System Using Hybrid ANFIS-FLOWER Pollination Optimization Algorithm

Neeraj Priyadarshi[1,*], Sanjeevikumar Padmanaban [2], Lucian Mihet-Popa [3], Frede Blaabjerg [4], and Farooque Azam[1]

[1] Department of Electrical and Electronics Engineering, Millia Institute of Technology, Purnea, India; neerajrjd@gmail.com, farooque53786@gmail.com
[2] Department of Energy Technology, Aalborg University, 6700 Esbjerg, Denmark; san@et.aau.dk
[3] Faculty of Engineering, Østfold University College, Kobberslagerstredet 5, 1671 Kråkeroy-Fredrikstad, Norway; lucian.mihet@hiof.no
[4] Center for Reliable Power Electronics (CORPE), Department of Energy Technology, Aalborg University, Aalborg, Denmark; fbl@et.aau.dk
* Correspondence: lucian.mihet@hiof.no; Tel.: +47-922-713-53

Abstract: In this research paper, a hybrid Artificial Neural Network (ANN)-Fuzzy Logic Control (FLC) tuned Flower Pollination Algorithm (FPA) as a Maximum Power Point Tracker (MPPT) is employed to emend root mean square error (RMSE) of photovoltaic (PV) modeling. Moreover, Gaussian membership functions have been considered for fuzzy controller design. This paper interprets Luo converter occupied brushless DC motor (BLDC) directed PV water pump application. Experimental responses certify the effectiveness of the suggested motor-pump system supporting diverse operating states. Luo converter is newly developed dc-dc converter has high power density, better voltage gain transfer and superior output waveform and able to track optimal power from PV modules. For BLDC speed controlling there is no extra circuitry and phase current sensors are enforced for this scheme. The recentness of this attempt is adaptive neuro-fuzzy inference system (ANFIS)-FPA operated BLDC directed PV pump with advanced Luo converter has not been formerly conferred.

Keywords: ANFIS, artificial neural network, brushless DC motor, FPA, maximum power point tracking, photovoltaic system, root mean square error.

---

1. Introduction

As the conventional energy sources are depleting day by day, the demand of renewable energy sources are raising with considered attention [1-3]. Solar energy sources are promising renewable energy sources for developed and developing nations due to free, abundant and environmental friendliness nature. The standalone photovoltaic (PV) systems for water pumping applications are employed for remote areas [4-5]. Because of grid absence in remote places the standalone PV water pumping is installed for agricultural and household applications. Various electric motors have been used to drive the pumping system [6-7]. The DC motor based pumping system requires maintenance because of commutator and brush presence. Therefore, DC motors are not frequently used for PV pumping applications. The single phase induction motors have also been used for driving low inertia torque load.

Preprints (www.preprints.org) | NOT PEER-REVIEWED | Posted: 19 March 2018 doi:10.20944/preprints201803.0158.v1

Peer-reviewed version available at Energies 2018, 11, 1067; doi:10.3390/en11051067

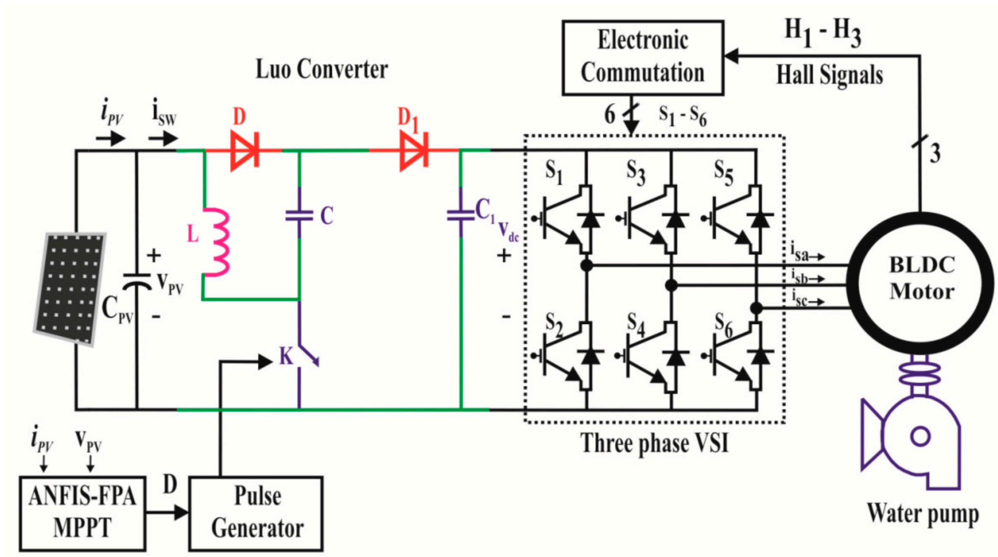

Figure 1 BLDC driven Photovoltaic Complete System Formation

Due to complex control strategy, the induction motors are not efficient for pumping applications. Therefore, in this research work Brushless DC (BLDC) motor has been considered as it has simple design control, low power range and require maintenance free operation compared to AC motors [8].

Distinct DC-DC converters were contend for optimizing PV module generated power with soft starting and controlling motor pump system [9-11]. The contemporary PV system has unsubstantial converse competency. Therefore, Maximum Power Point Trackers (MPPT) is the indispensable constituents required for optimal power tracking from PV modules. In contrast with different employed power converters, modern Luo converter has been considered for this research approach as it delivers better power/ density ratio with economical implementation [20]. Numerous MPPT methods have been occupied viz. Perturb and Observe (P&O), Increment Conductance (INC), Fraction Short/Open circuit etc. [12-14]. Under steady state operating conditions particular algorithms provide high outturn. But these algorithms are found lacking under adverse weather conditions with slow convergence velocity and unable to achieve global power point (GPP) for partial shading situations with high power oscillations around this point. Recently different intelligent techniques viz. Fuzzy Logic Control (FLC), Artificial Neural Network (ANN) has been employed for PV tracking [15]. However, because of complex fuzzy inference rules and individual sensor requirements, meta-heuristic algorithms have been employed nowadays. Genetic algorithm and artificial Immune system are meta-heuristic algorithms used for non-linear stochastic problem solution. However, the implementation of selection, mutation and crossover process is complex with reduced convergence computational period. Currently, Bio-inspired and swarm optimization have been derived as MPPT techniques. The particle swarm optimization is an evolutionary methodology based on nature of swarm is able to reduce oscillations around GMPP [16-18]. Nevertheless, variance of this algorithm is capitulated when randomness is miniaturized. Surrogating to swarm techniques, currently bio-inspired algorithms viz. Firefly Algorithms (FA), Artificial Bee Colony (ABC), Cuckoo Search etc. have been considered as bio-inspired MPPT and has advantage of high convergence speed, less transient with fast tracked performance. However, the implementation complexities with tuning of parameters are the major hindrance of this finding. Included work, a novel flower pollination algorithm is contemplated and associated with hybrid ANFIS MPPT algorithm. The hybrid ANFIS-Flower Pollination Algorithm (FPA) [19] has simple implementation, high convergence speed with tune parameters and easier code compilation are the major merits. The recentness of this research work is

Preprints (www.preprints.org) | NOT PEER-REVIEWED | Posted: 19 March 2018 doi:10.20944/preprints201803.0158.v1

Peer-reviewed version available at Energies 2018, 11, 1067; doi:10.3390/en11051067

BLDC drive PV pumping employed Luo converter [20] with hybrid ANFIS-FPA have not been conferred and examined using dSPACE (DS1104) platform under changing weather conditions.

2. Complete System Formation

Fig 1 illustrates the Luo converter employed BLDC driven PV pumping for remote location. A hybrid ANFIS-FPA MPPT controller is operated to produce required pulse for power switched of Luo converter. This converter delivers better power/ density ratio with economical implementation with interface between inverter power circuit and solar system. Moreover, electronic commutation methodology controls voltage source inverter (VSI) employed BLDC motor in which winding current is adjusted with the help of decoder in proper sequence.

2.1 PV Generator

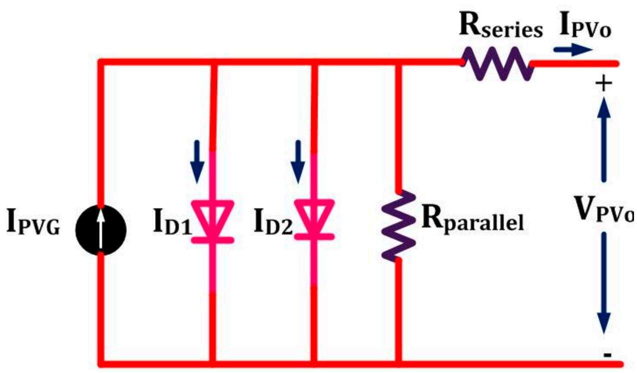

Figure 2 Two diode PV cell model

In this research work a two diode PV cell model is considered (Figure 2) because of simple and accurate model compared to single diode PV cell. By means of photoelectric effect, the conversion of solar to electricity takes place and output power can be enhanced by connecting numerous solar cells in shunt or series as per requirement. Both diodes employed to represent polarization occurrence with current source exhibiting sun insolation followed by power loss delivered by resistances (series/shunt) used. The prognosis of overall system is calculated on the basis of accurate equivalent modeling. The output of PV current is expressed mathematically as:

$$I_{PVo} = I_{PVG} - I_{RSC}(I' + 2) - \left(\frac{V_{PVo}+I_{PVo}*R_{series}}{R_{Parallel}}\right) \quad (1)$$

Where,

$$I' = \exp\left(\frac{V_{PVo}+I_{PVo}*R_{series}}{V_{Thermal}}\right) + \exp\left(\frac{V_{PVo}+I_{PVo}*R_{series}}{A*V_{Thermal}}\right) \quad (2)$$

I_{PVG} = Photo Current

I_{RSC} = Diode reverse saturation current

I_{PVO} = Output PV current

V_{PVO} = PV output voltage

R_{series} = Resistance in series

Peer-reviewed version available at Energies 2018, 11, 1067; doi:10.3390/en11051067

$V_{Thermal}$ = PV module thermal voltage

A = Ideality constant of diode

2.2 Luo Converter

Renewable technology comprises dc-dc topologies for yield of energy harvest with admissible proficiency. With respect to other dc-dc converters, modern Luo topology depicted in Fig 3 delivers reasonable cost, better power/ density ratio and enhanced transformation efficiency. It comprises least ripple content with geometric output voltage and surpasses the parasitic element action. The auxiliary benefit of this topology is switched components are taken ground as a reference. In addition to that the input inductor smoothes the ripple present to input source. Employed capacitors get charged to stated value to accomplish high voltage leveled.

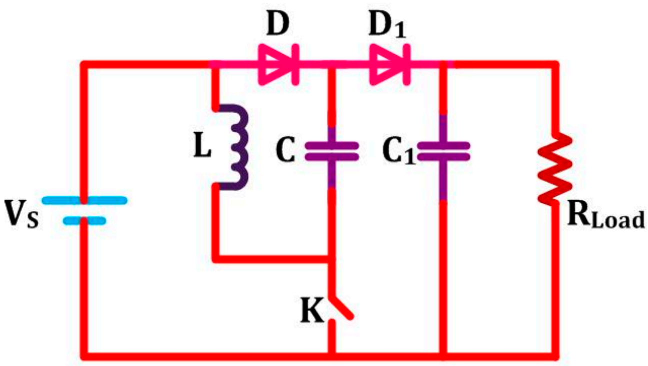

Figure 3 Power Circuit Luo converter

Transfer gain voltage is evaluated as:

$$\frac{V_0}{V_S} = \frac{2 - d_{duty}}{1 - d_{duty}} \tag{3}$$

Relation between inductor ripple current and duty cycle is expressed as:

$$\Delta I_{L_{Ripple}} = \frac{V_S * d_{duty}}{f_{Pulse} * L} \tag{4}$$

Capacitors (C=C_1) values are determined mathematically as:

$$C = C_1 = \frac{(1 - d_{duty}) * V_0}{f_{Pulse} * R_{Load} * \Delta V_0} \tag{5}$$

Where, d_{duty}= Duty ratio

f_{Pulse}= Frequency of Switched pulse

2.3 A Hybrid Proposed FLC-ANN tuned FPA MPPT

In this proposed scheme, hybrid ANFIS-FPA MPPT algorithm is realized for maximizing PV outturn and accurate motion control with PV-pump interface. The FLC data is trained by ANN which finally optimized by FPA method lead to minimum RMSE of FLC and ANN. It comprises the dominance of FLC and ANN both. The threshold and weight of NN models are optimized by FPA algorithm to produce

Preprints (www.preprints.org) | NOT PEER-REVIEWED | Posted: 19 March 2018 doi:10.20944/preprints201803.0158.v1

Peer-reviewed version available at Energies 2018, 11, 1067; doi:10.3390/en11051067

123 minimum RMSE. Figure 4 depicts the complete structure of hybrid learning in which learning data has
124 been achieved from FLC architecture.

125 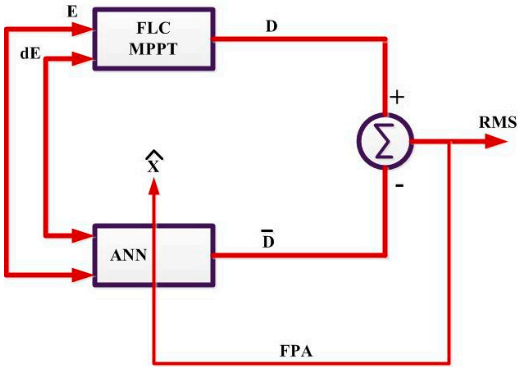

126 Figure 4 complete structure of hybrid ANFIS-FPA

127 The FLC architecture comprises fuzzification, Inference Rule base and defuzzification as elemental
128 constituents. Real variables are converted to linguistic parameters using fuzzification. The requisite
129 output introduced by Mamdani fuzzy inference rule deployed by max-min composition. With the help of
130 centroid method, the defuzzification process converts the linguistic parameters to real values. Employed
131 membership values are illustrated by Fig 5.

132 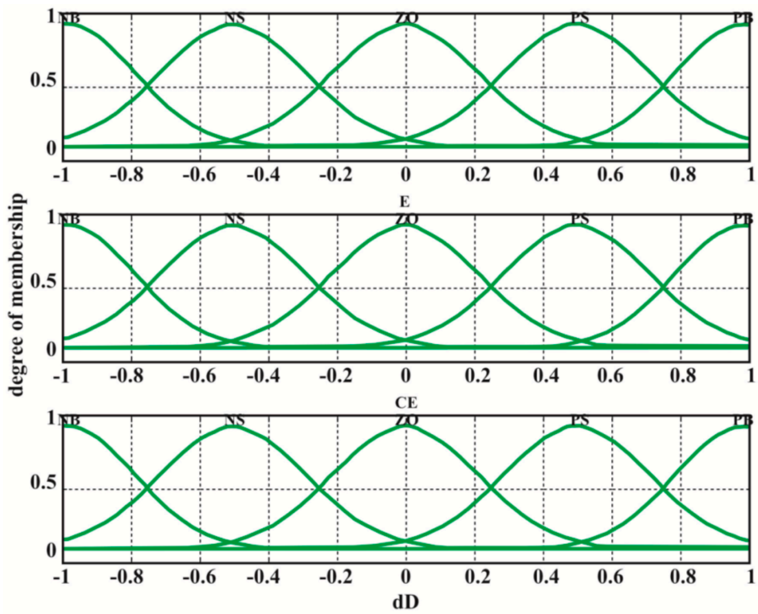

133 Figure 5 Employed membership values

134 The ANN objective function is expressed mathematically as:

135 $$\text{RMSE} = \left[\frac{1}{P}\sum_{i=1}^{P}(Y_F - Y_N)^2\right]^{1/2} \quad (6)$$

136 Where,

137 P =Total Sample

Preprints (www.preprints.org) | NOT PEER-REVIEWED | Posted: 19 March 2018 doi:10.20944/preprints201803.0158.v1

Peer-reviewed version available at Energies 2018, 11, 1067; doi:10.3390/en11051067

Y_F = Fuzzy output

Y_N = Neural Network output

FPA method of MPPT is predicted by reproduction of flower of transferring pollen. This convection is possible through biotic/cross and abiotic/self pollination. In cross pollination the pollens are translated between two unlike flowers. On the other hand abiotic pollination takes place between distant species. It is noted that in flower pollination 90% possibility of cross pollination and only 10% possibility of self pollination happen which is limited in the probability range R ε [1, 0]. The complete process is based on following rules:

Rule I: The biotic pollination use levy flight for transferring pollens and called global pollination in which i^{th} pollen solution vector is expressed mathematically as:

$$X_i^{T+1} = X_i^T + L_f * \left(X_i^T - G_{best}\right) \quad (7)$$

Where,

X_i^T = Vector representing solution

T = No. of iteration

L_f = Levy flight factor

G_{best} = Global best solution

Rule II: Self pollination is termed as local pollination and characterized mathematically as:

$$X_i^{T+1} = X_i^T + P_f * (X_m^T - X_n^T) \quad (8)$$

X_m^T and X_n^T= two unlike pollen in the species

P_f = Switched probability

Rule III: The performance of flower is assumed identical to the probability of reproduction that equivalent with resemblance of two concerned flowers.

Rule IV: The pollination is interchanged within global to local depends on switching probability lies at interval between 0 and 1.

2.4 Electronic BLDC Commutator and VSI switching

Commutation in Permanent Magnet DC Motor (PMDC) is obtained by commutator and brushes. Nevertheless, hall sensors are important component employed in BLDC motor which senses the position of rotor as a commutation wave. Coils and permanent magnet are employed as a stator and rotor respectively in which stator's magnetic field rotates rotor. Armature of BLDC motor consists of permanent magnet as a substitute of coil which does not require brushes. Figure 6 demonstrates BLDC driven structure with induced EMF and reference current.

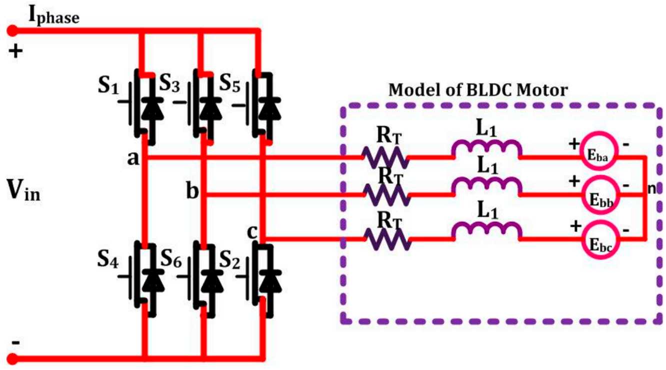

(a)

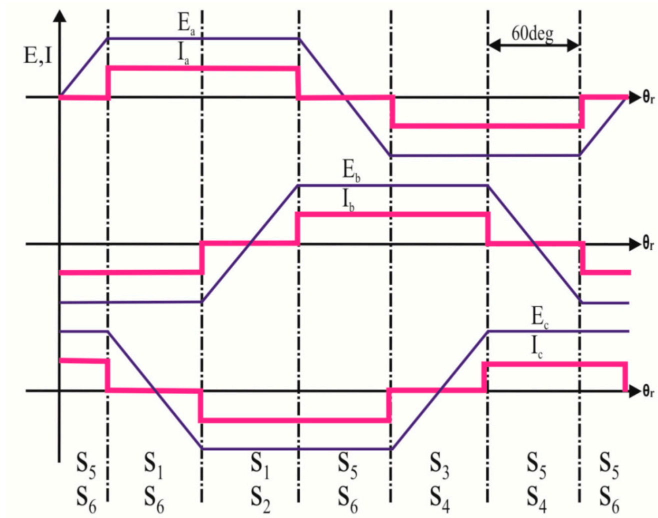

(b)

Figure 6 BLDC driven structure with induced EMF and reference current

The BLDC motor is analyses mathematically as:

$$\begin{bmatrix} V_{ap} \\ V_{bp} \\ V_{cp} \end{bmatrix} = \begin{bmatrix} R_T & 0 & 0 \\ 0 & R_T & 0 \\ 0 & 0 & R_T \end{bmatrix} \begin{bmatrix} I_{ap} \\ I_{bp} \\ I_{cp} \end{bmatrix} + \begin{bmatrix} L_1 - M_1 & 0 & 0 \\ 0 & L_1 - M_1 & 0 \\ 0 & 0 & L_1 - M_1 \end{bmatrix} \frac{d}{dx} \begin{bmatrix} I_{ap} \\ I_{bp} \\ I_{cp} \end{bmatrix} + \begin{bmatrix} E_{ba} \\ E_{bb} \\ E_{bc} \end{bmatrix} \quad (9)$$

Developed electromagnetic torque by BLDC motor can be expressed mathematically as:

$$T_{EM} = \frac{E_{ba} * I_{ap} + E_{bb} * I_{bp} + E_{bc} * I_{cp}}{\omega_{rotor}} \quad (10)$$

Where,

V_{ap}, V_{bp}, V_{cp}= Phase voltage of a 3-Phase BLDC motor

I_{ap}, I_{bp}, I_{cp}= Phase Currents

E_{ba}, E_{bb}, E_{bc}= Phase Back EMF of BLDC motor

Preprints (www.preprints.org) | NOT PEER-REVIEWED | Posted: 19 March 2018 doi:10.20944/preprints201803.0158.v1

Peer-reviewed version available at *Energies* **2018**, *11*, 1067; doi:10.3390/en11051067

L_1 = Each Phase self-inductance

M_1 =Two phase's mutual inductance

T_{EM} = Developed Electromagnetic torque of BLDC motor

ω_{Rotor} = Rotor Speed

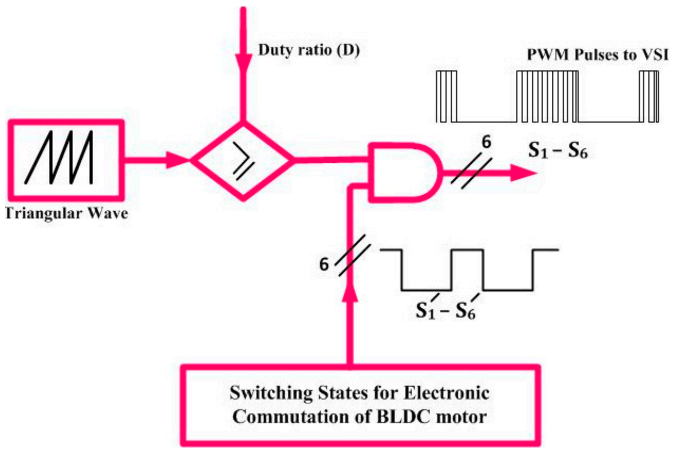

Figure 7 gating signal for 3-phase VSI

Electronic commutation process is used to control the VSI employed BLDC motor in which winding current is adjusted with the help of decoder in proper sequence. In this method, symmetrical DC currents are situated to the phase voltage at 120º. Based on the motor alignment, the hall sensors produces signals of 60º phase difference. The gating signal for 3-phase VSI is generated by transforming hall signals using decoder is illustrated by Fig 7. The pulse width modulated pulses are generated by comparing triangular signal with duty cycle produced through MPPT. Table 1 portrays Hall signals and Switching states of BLDC used with Electronic commutation.

Table 1 Hall signals and Switching states

Angle	**Hall Signals**			**Switching States**					
	H_1	**H_2**	**H_3**	**s_1'**	**s_2'**	**s_3'**	**s_4'**	**s_5'**	**s_6'**
0 - $\pi/3$	1	0	1	0	1	1	0	0	0
$\pi/3$ - $2\pi/3$	0	0	1	0	1	0	0	1	0
$2\pi/3$ - π	0	1	1	0	0	0	1	1	0
π - $4\pi/3$	0	1	0	1	0	0	1	0	0
$4\pi/3$ - $5\pi/3$	1	1	0	1	0	0	0	0	1
$5\pi/3$ - 2π	1	0	0	0	0	1	0	0	1

The high frequencies PWM pulses and six fundamental signals are operated with AND gate, which produces 6 gating pulses for VSI inverter. As the atmospheric conditions changes, the duty cycle is also regulated using MPPT methods which controls the VSI and finally the BLDC motor is adjusted accordingly.

3. Experimental Results

Peer-reviewed version available at *Energies* **2018**, *11*, 1067; doi:10.3390/en11051067

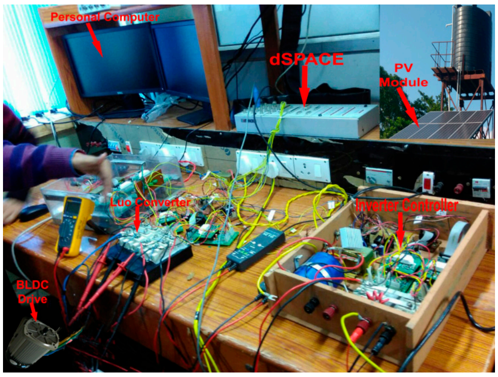

Figure 8 BLDC driven Luo converter employed PV pumping hardware developed

Performance justification of BLDC driven PV pumping employed Luo converter has been done through dSPACE controller. For purpose of MPPT operation, LA-55/LV-25 as current/voltage sensors is employed during practical implementation. Fig 8 portrays the BLDC driven Luo converter employed PV pumping hardware developed in the laboratory. With the help of A/D converter, analog pulses are transformed to digital and fed to dSPACE interface. Electronic commutation/Controlling BLDC has been executed by obtained hall pulses from input/output terminal and then generated pulses are outturned to inverter.

3.1 Steady State Performance

The experimental behaviors of PV module and motor pumping system have been tested under steady state condition of irradiance level 1000w/m². The proposed MPPT design technique is working effectively and tracks optimal power from PV module with unity duty cycle at 1000 W/m² solar insolation level depicted in Fig 9. The corresponding BLDC motor and torque (1500 rpm) has been demonstrated in Fig 9 (d) presents the obtained hall sensor pulses with motor torque. The performance of BLDC motor-pumping system has been evaluated with 300 W/m² solar irradiance. The motor torque is experimentally obtained which is sufficient to operate PV water pumping. Based on duty cycle generation using MPPT algorithm, the corresponding hall signals have been generated to trigger six switches of inverter.

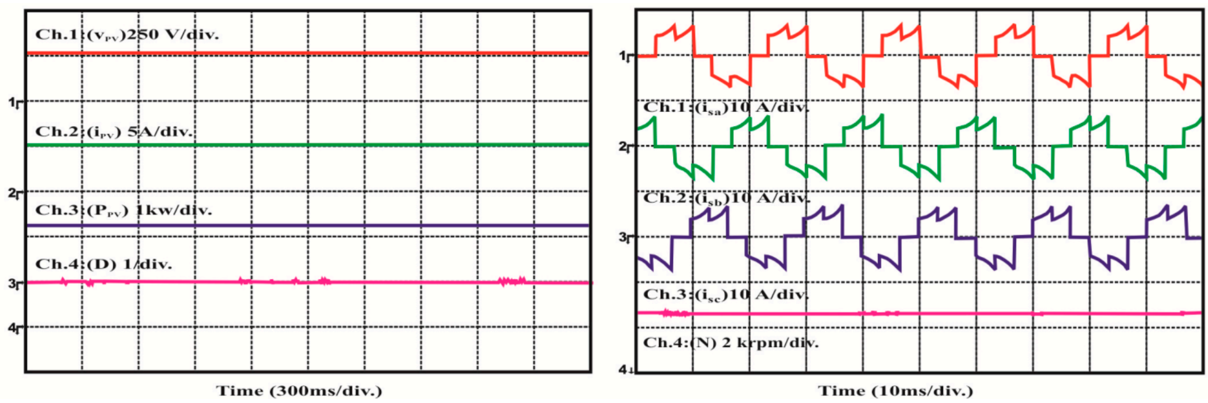

(a) (b)

Preprints (www.preprints.org) | NOT PEER-REVIEWED | Posted: 19 March 2018 doi:10.20944/preprints201803.0158.v1

Peer-reviewed version available at *Energies* **2018**, *11*, 1067; doi:10.3390/en11051067

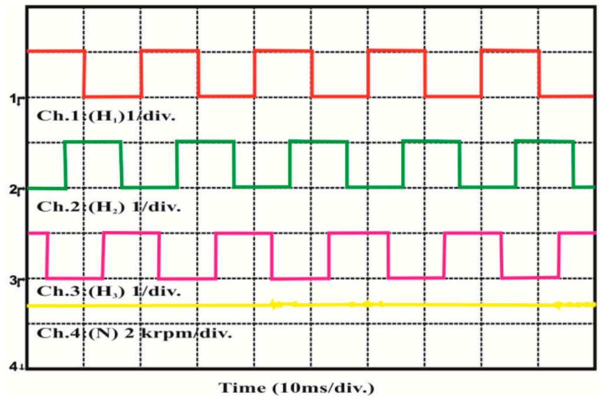

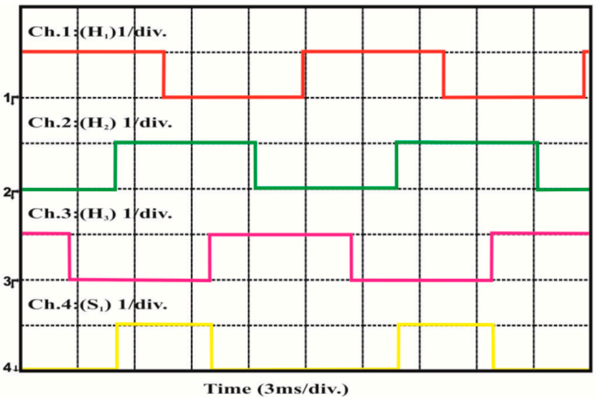

(c) (d)

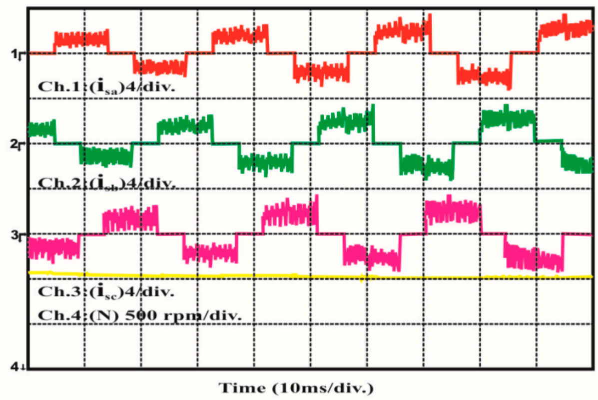

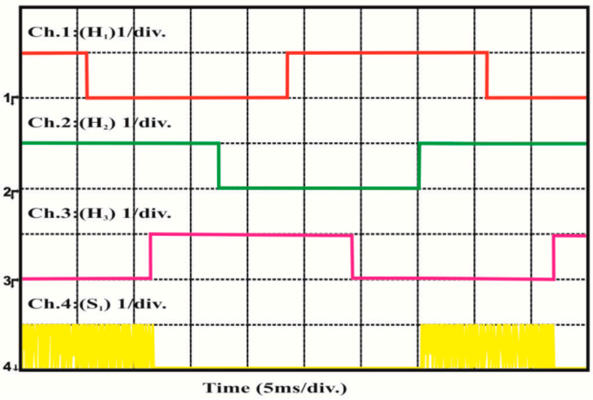

(e) (f)

Figure 9 BLDC driven Luo converter employed PV pumping (a) PVG at 1000 W/m^2 (b) BLDC performance at 1000 W/m^2 (c) generated hall sensor pulses at 1000 W/m^2 (d) switched and hall pulses at 1000 W/m^2 (e) BLDC performance at 300 W/m^2 (f) switched and hall pulses at 300 W/m^2

3.2 Dynamic Behavior of PV system

The effective practice of recommended PV pumping system was proved under varying sun insolation level. In this experiment, solar irradiance level is varied from 300W/m^{2}to 1000W/m^2. According to variation in sun irradiance level , corresponding changes in PV current, DC link voltage , BLDC stator current and motor torque have been verified (Fig 10) and PV pumping is running without any interruption. The duty cycle for BLDC-PV pump control is generated with variation in sun insolation accordingly and outstanding motion control has been comprehended.

Preprints (www.preprints.org) | NOT PEER-REVIEWED | Posted: 19 March 2018 doi:10.20944/preprints201803.0158.v1

Peer-reviewed version available at *Energies* **2018**, *11*, 1067; doi:10.3390/en11051067

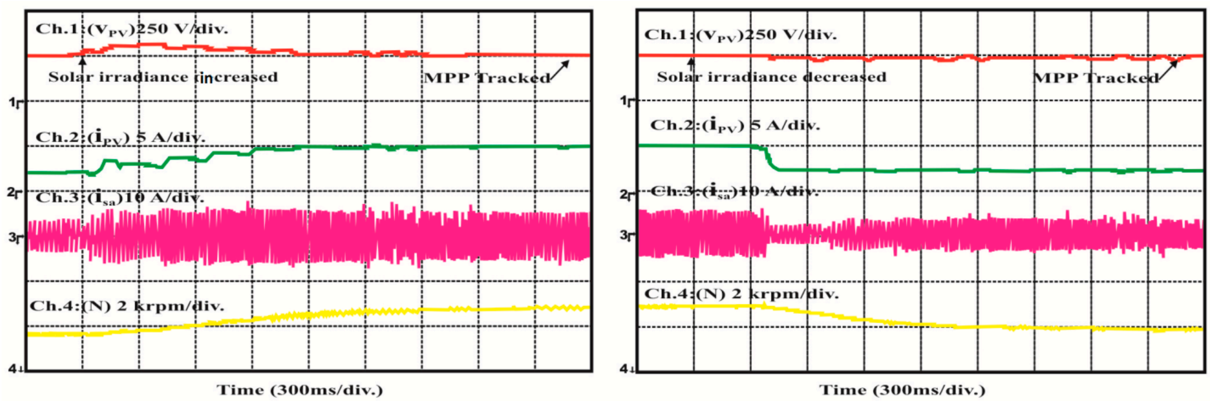

(a) (b)

Figure 10 BLDC driven Luo converter (a) increased solar irradiance (b) decreased solar irradiance

3.3 Behavior at Starting

Practical results found in Fig 11 interpret the safe starting of BLDC motor under irradiance level 1000W/m² and 300W/m². Initially the duty cycle is kept 0.5 to run the motor. The sufficient motor speed is obtained by controlling the starting current which runs the motor-pump system successfully. Fig 11portrays the successful action of BLDC-PV pump at start by limiting starting current which reveals the progression with safe and soft started.

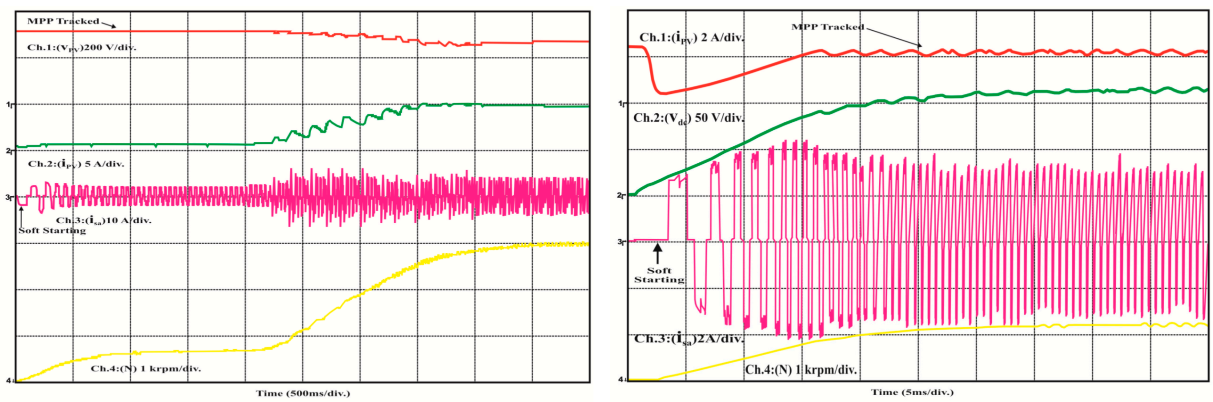

(b) (b)

Figure 11 BLDC driven Luo converter employed PV pumping under soft starting (a) 1000 W/m² (b) 400 W/m²

Table 2 Laboratory adopted BLDC specification

S.N	Parameters	Value
1.	Resistance of stator	4.16Ω
2.	Inductance value of stator	2.2 mH
3.	Speed rating	1500rpm
4.	Number of Pole pair	2

Preprints (www.preprints.org) | NOT PEER-REVIEWED | Posted: 19 March 2018 doi:10.20944/preprints201803.0158.v1

Peer-reviewed version available at Energies 2018, 11, 1067; doi:10.3390/en11051067

5.	Constants(Voltage & torque)	$86V_{LL}$/KRPM & 0.85 Nm/Ampere

Table 2 portrays laboratory adopted BLDC specification for motion control PV pump. Fig 12 interprets the existent global nature of PV system under divergent sun radiation which is demonstrated by dark line. The operation begins with $V_{OPEN\ Ckt}$ state and reaches to global power point with variable solar irradiance. With application of hybrid ANFIS-FPA MPPT, steady GMP is attained over a complete day.

The performance of MPPT controllers are tested with stepped irradiance input. Under these situations, ANFIS-FPA has high tracked PV power with proportionately lesser GMP time. Practical results demonstrate that ANFIS-FPA algorithm contributes rapid and insignificant swinging differentiated with FPA MPPT illustrated by Fig 13 (a) and (b).

Fig 14 demonstrates the behavior of numerous MPPT control under standard test conditions. A hybrid ANFIS-FPA algorithm has global power point trajectory with utmost PV tracked power and has zero oscillation throughout equated with different controllers. The PV tracked trajectories are also examined under fluctuating weather situations (Fig 15). Practical results reveal that ANFIS-FPA optimized MPPT provides optimal tuning with high performance index.

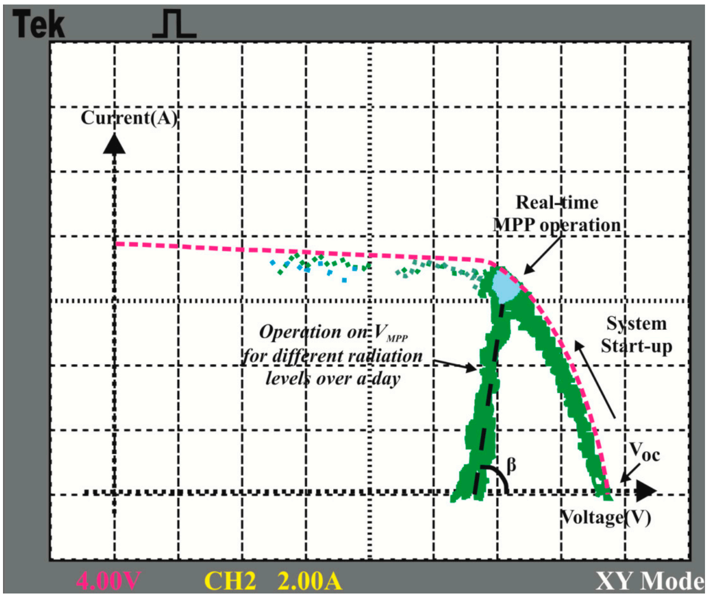

Figure 12 Existent global nature of PV system under divergent sun radiation

Preprints (www.preprints.org) | NOT PEER-REVIEWED | Posted: 19 March 2018 doi:10.20944/preprints201803.0158.v1

Peer-reviewed version available at Energies 2018, 11, 1067; doi:10.3390/en11051067

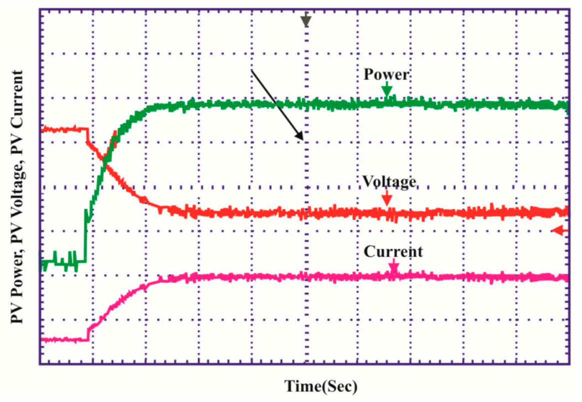

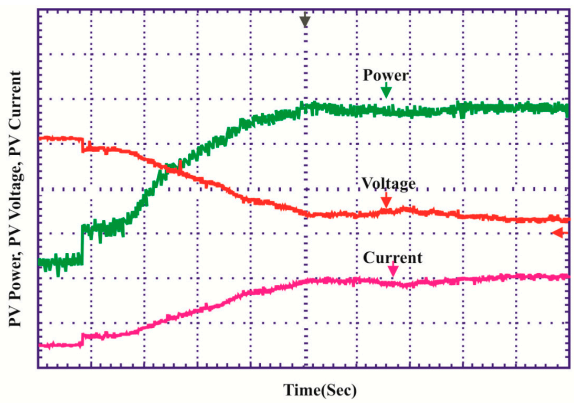

(a) (b)

Figure 13 Behavior of MPPT under stepped irradiance (a) Hybrid ANFIS-FPA (b) FPA

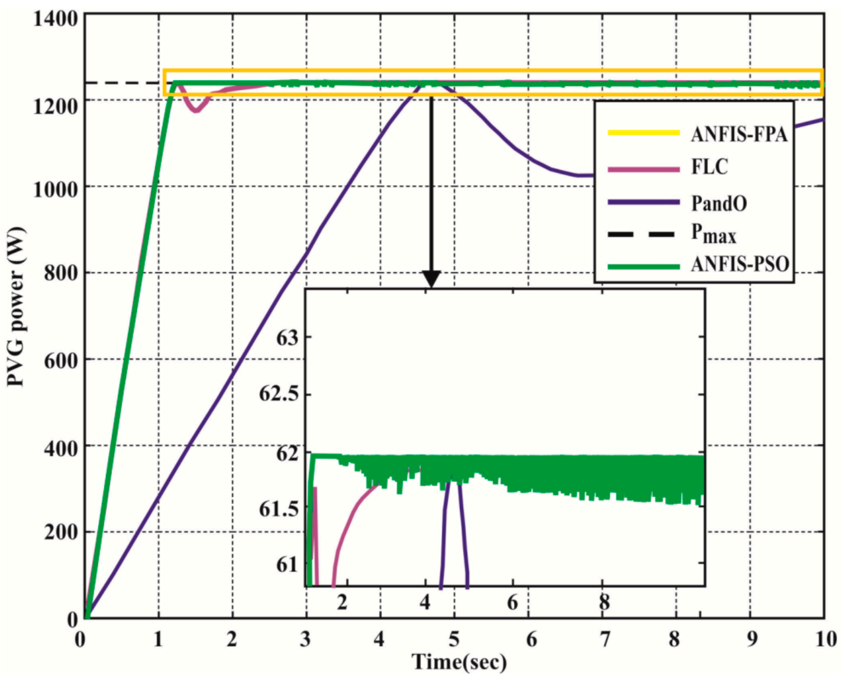

Fig 14 Behavior of numerous MPPT control under standard test conditions

Preprints (www.preprints.org) | NOT PEER-REVIEWED | Posted: 19 March 2018 doi:10.20944/preprints201803.0158.v1

Peer-reviewed version available at *Energies* **2018**, *11*, 1067; doi:10.3390/en11051067

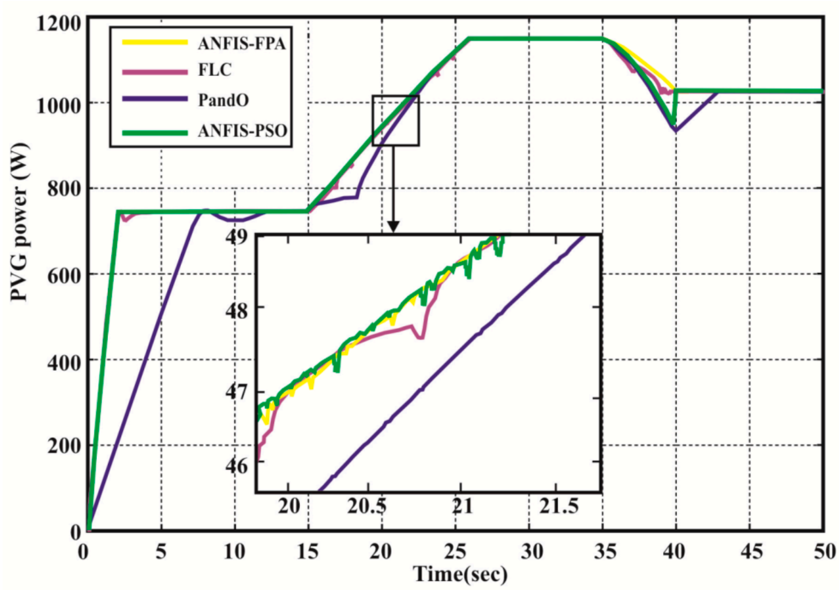

Figure 15 PV tracked trajectories examined under fluctuating weather situations

4 Conclusion

The Luo converter based BLDC driven PV pumping with ANFIS-FPA MPPT has been demonstrated under varying weather conditions using dSPACE platform. The Luo converter has been proposed for desired GMP functions. The PV fed BLDC motor drive pumping system operates effectively under steady, dynamic state and soft starting operating conditions which validated through experimentally obtained responses. The enforcement of ANFIS-FPA MPPT controller has been equated with general P&O and ANFIS-PSO method which gives high tracking efficiency, fast design and rapid convergence time under varying solar irradiance level.

Author Contributions: All authors contributed equally for the decimation of the research article in current form.

Conflicts of Interest: The authors declare no conflict of interest.

References

[1] Jedari M, fathi S H. A New Approach for Photovoltaic Arrays Modeling and Maximum Power Point Estimation in Real Operating Conditions. IEEE Trans. on Ind. Electron. 2017; 64(12): 9334 – 9343.

[2] Aamri F EL, Maker H, Sera D, Spataru S, Guerrero J M, Mouhsen A. A Direct Maximum Power Point Tracking Method for Single-Phase Grid Connected PV Inverters. IEEE Trans. on Power Electron. 2017; (99): 1-10.

[3] Tiwari S K, Singh B, Goel P K. Design and Control of Autonomous Wind-Solar System with DFIG Feeding 3-Phase 4-Wire Loads. IEEE Trans. on Ind. Appl. 2017; (99): 1-8.

[4] Kumar R, Singh B. BLDC Motor Driven Solar PV Array Fed Water Pumping System Employing Zeta Converter. IEEE Trans. on Ind. Appl. 2016; 52(3): 2315 – 2322.

[5] Montorfano M, Sbarbaro D, Mor´an L. Economic and technical evaluation of solar assisted water pump stations for mining applications: A case of study. IEEE Trans. on Ind. Appl. 2016; 52(5): 4454 – 4459.

Peer-reviewed version available at *Energies* **2018**, *11*, 1067; doi:10.3390/en11051067

[6] Alghuwainem S M. Speed Control of a PV Powered DC Motor Driving a Self- Excited 3-Phase Induction Generator for Maximum Utilization Efficiency. IEEE Trans. on Energy Conversion. 1996; 11(4): 768-773.
[7] Jain S, T K A, Karampuri R, Somasekhar V T. A Single-Stage Photo Voltaic System for a Dual-Inverter fed Open-End Winding Induction Motor Drive for Pumping Applications. IEEE Trans. on Power Electron. 2015; 30(9): 4809 - 4818.
[8] Sashidhar S, Fernandes B G. A Novel Ferrite SMDS Spoke-Type BLDC Motor for PV Bore-Well Submersible Water Pumps. IEEE Trans. on Power Electron. 2017; 64(1): 104-114.
[9] Killi M, Samanta S. An Adaptive Voltage Sensor Based MPPT for Photovoltaic Systems with SEPIC Converter including Steady State and Drift Analysis. IEEE Trans. on Power Electron. 2017; 64(1): 104-114.2015; 62(12): 7609 – 7619.
[10] Priyadarshi N, Kumar V, Yadav K, Vardia M. An Experimental Study on Zeta buck-boost converter for Application in PV system. Hand book of distributed generation. DOI10.1007/978-3-319-51343-0_13.
[11] Priyadarshi N, Anand A, Sharma A K, Azam F, Singh V K, Sinha R K. An Experimental Implementation and Testing of GA based Maximum Power Point Tracking for PV System under Varying Ambient Conditions Using dSPACE DS 1104 Controller. Int. Journal of Renewable Energy Research, 2017; 7(1): 255-265.
[12] Kumar N, Hussain I, Singh B, Panigrahi B K. Framework of Maximum Power Extraction from Solar PV Panel using Self Predictive Perturb and Observe Algorithm. IEEE Trans. on Sustainable Energy. 2017; (99): 1-9.
[13] Elgendy M A, Zahawi B, Atkinson D J. Assessment of the Incremental Conductance Maximum Power Point Tracking Algorithm. IEEE Trans. on Sustainable Energy. 2013; 4(1): 108-117.
[14] Zamora A C, Vazquez G, Sosa J M, Rodriguez P R M, Juarez M A. Efficiency Based Comparative Analysis of Selected Classical MPPT Methods. IEEE Int. Autumn Meeting on Power, Electronics and Computing. 2017; 1-6.
[15] Abu-Rub H, Iqbal A, Ahmed SK M, Peng F Z, Li Y, Baoming G. Quasi-Z-Source Inverter-Based Photovoltaic Generation System With Maximum Power Tracking Control Using ANFIS. IEEE Trans. on Sustainable Energy. 2013; 4(1): 11-20.
[16] Priyadarshi N, Sharma A K, Azam F. A Hybrid Firefly-Asymmetrical Fuzzy Logic Controller based MPPT for PV-Wind-Fuel Grid Integration. Int. Journal of Renewable Energy Research. 2017; 7(4): 1546-1560.
[17] Sundareswaran K, Sankar P, Nayak P S R, Simon S P, Palani S. Enhanced Energy Output From a PV System Under Partial Shaded Conditions Through Artificial Bee Colony. IEEE Trans. on Sustainable Energy 2015; 6(1): 198-209.
[18] Kalaam R N, Muyeen S M , Al-Durra A, Hasanien H N, Al-Wahedi K. Optimisation of controller parameters for grid tied photovoltaic system at faulty network using artificial neural network-based cuckoo search algorithm. IET Renewable Power Gen. 2017; 11(12): 1517-1526.
[19] Ram J P, Rajasekar N. A novel Flower Pollination based Global Maximum Power Point method for Solar Maximum Power Point Tracking. IEEE Trans. on Power Electron. 2017; 32(11): 8486 – 8499.
[20] Pansare C, Sharma S K, Jain C, Saxena R. Analysis of a Modified Positive Output Luo Converter and its application to Solar PV system. IEEE Ind. Appl. 2017; 1-6.